Stubbe, J., & Abeles, R. H. (1977) *J. Biol. Chem. 252*, 8338.
Ulm, E. H., Sweet, C. S., Duggan, D. E., & Minsker, D. H. (1979) *Fed. Proc., Fed. Am. Soc. Exp. Biol. 38*, 1021 (Abstr.).
Walsh, C. T. (1977) in *Horizons in Biochemistry & Biophysics* (Quagliariello, E., Palmieri, F., & Singer, T. P., Eds.) Vol. 3, p 36, Addison-Wesley, Reading, MA.
Walsh, C., Johnston, M., Marcotte, P., & Wang, E. (1978) in *Enzyme-Activated Irreversible Inhibitors* (Seiler, N., Jung, M. J., & Koch-Weser, J., Eds.) p 177, Elsevier/North-Holland Biomedical Press, Amsterdam.
Wang, E., & Walsh, C. (1978) *Biochemistry 17*, 1313.
Weber, K., & Osborn, M. (1969) *J. Biol. Chem. 244*, 4406.
Weissbach, H., Lovenberg, W., & Udenfriend, S. (1960) *Biochem. Biophys. Res. Commun. 3*, 225.
Yamada, H., & O'Leary, M. H. (1977) *J. Am. Chem. Soc. 99*, 1660.
Yamada, H., & O'Leary, M. H. (1978) *Biochemistry 17*, 669.

Comparison of the Zinc Binding Domains in the 7S Nerve Growth Factor and the Zinc–Insulin Hexamer†

Michael F. Dunn,* Scott E. Pattison,‡ Michael C. Storm, and Edward Quiel§

ABSTRACT: The chromophoric divalent metal ion chelator 2,2′,2″-terpyridine (Terpy) is used as a kinetic and spectroscopic probe to investigate the zinc binding domains in the mouse 7S nerve growth factor protein (7S NGF_n) and the zinc–insulin hexamer $(In)_6(Zn^{2+})_2$. The stopped-flow rapid-mixing kinetic time courses for the sequestering and removal of zinc ion from both of these zinc metalloprotein hormones are remarkably biphasic. The fast phase of each reaction is second order overall: first order in Terpy and first order in protein-bound zinc ion. Although the spectral changes associated with the slow phase correspond to the uptake of 1 mol of Terpy per g-atom of zinc ion, the slow phase is a first-order process (zero order in Terpy). The concentration dependencies and spectral changes are consistent with a common reaction mechanism for both proteins; the fast phase involves the formation of a mono(Terpy)–Zn(II)–protein complex at each zinc site, and the slow phase involves the rate-limiting dissociation of the Terpy-bound zinc ions from the protein, followed by the rapid coordination of a second Terpy molecule and formation of the bis(Terpy)–Zn(II) complex. In contrast, the reactions of Terpy with carboxypeptidases A and B, carbonic anhydrase, thermolysin, and horse liver alcohol dehydrogenase all were very slow ($t_{1/2}$ of hours to days). In each case, the time course was described by a single exponential. The high-resolution X-ray structure of $(In)_6(Zn^{2+})_2$ [Blundell, T., Dodson, G., Hodgkin, D., & Mercola, D. (1972) *Adv. Protein Chem. 26*, 279] provides a satisfying structural rationale for the biphasic time course. Each of the two zinc ions is hexacoordinate. Three of the ligands are water molecules; the remaining three are imidazolyl moieties of His-B10. Based on this structural information, we conclude that the rapid phase of the reaction involves displacement of the three water molecules by the tridentate Terpy. The striking similarities between the reactions of 7S NGF_n and $(In)_6(Zn^{2+})_2$ with Terpy suggest the existence of structural similarity in the zinc binding domains of 7S NGF_n and $(In)_6(Zn^{2+})_2$.

The distantly related hormones nerve growth factor (NGF)[1] and insulin (In) both exist in dissociative equilibrium with free protomers under physiological conditions (Server & Shooter, 1977; Blundell et al., 1972). Zinc ion strongly shifts the equilibrium for each system toward the oligomeric state (Pattison & Dunn, 1975, 1976a,b; Au & Dunn, 1977; Grant et al., 1971; Goldman & Carpenter, 1974; Jeffrey, 1974; Blundell et al., 1972).

The native NGF oligomer (a 140000 M_r species, designated 7S NGF_n) appears to be a hexamer made up of three different classes of subunits (designated α, β, and γ) and contains two zinc ions. The γ subunit is a trypsin-like protease, and the β subunit contains the growth promoting activity, while the α subunit has no well-defined biological activity. The proteolytic activity of the γ subunit is completely inhibited in the 7S NGF_n species. Removal of zinc ion from the oligomer brings about full activation of the γ-subunit proteolytic activity (Pattison & Dunn, 1975, 1976a,b; Au & Dunn, 1977). The β subunit consists of two identical polypeptide chains made up of 118 amino acids each. The sequence of the β chain has been found to exhibit approximately 20–25% sequence homology with human proinsulin (Frazier et al., 1972; Angeletti & Bradshaw, 1971). Zinc ion binds to the 7S NGF oligomer with an apparent dissociation constant of 10^{-10}–10^{-11} M (Pattison & Dunn, 1976b).

Insulin in the presence of limited amounts of zinc ion forms a hexamer (constructed as a trimer of dimers) containing two zinc ions, hereafter designated as $(In)_6(Zn^{2+})_2$ (Blundell et al., 1972). In the presence of zinc ion, proinsulin also forms a hexamer containing 2 g-atoms of zinc ion (Frank & Veros, 1970; Pekar & Frank, 1972). The X-ray structure of $(In)_6(Zn^{2+})_2$ shows the two zinc ions are related by three twofold symmetry axes, and they are located on a threefold symmetry axis through the molecule. The two zinc ions are separated by an internal, water-filled cavity which forms a core about which the protomers are situated. Each of the two zinc ions is hexacoordinate (Blundell et al., 1972). The six inner sphere ligands are positioned in an octahedral array. Three of the

† From the Department of Biochemistry, University of California, Riverside, Riverside, California 92521. *Received April 3, 1979; revised manuscript received September 10, 1979.* Portions of this work were supported by American Cancer Society Grant DT-4 (National Division) and National Science Foundation Grant BNS-76-20218.

‡ Present address: Department of Chemistry, California Polytechnic Institute, Pomona, CA 91768.
§ Present address: School of Medicine, University of California, San Diego, La Jolla, CA 92093.

[1] Abbreviations used: 7S NGF_n and 7S NGF_a, the native and chelator-activated mouse submaxillary nerve growth factor proteins; In and $(In)_6(Zn^{2+})_2$, the insulin monomer and hexamer, respectively; Terpy, 2,2′,2″-terpyridine; Tris, 2-amino-2-(hydroxymethyl)-1,3-propanediol.

0006-2960/80/0419-0718$01.00/0

six ligands (histidylimidazolyl moieties of His-B10) are derived from each insulin dimer, while the remaining three ligands appear to be water molecules. The binding of zinc ion in the $(In)_6(Zn^{2+})_2$ complex is described by an apparent dissociation constant of approximately 10^{-6} M (Goldman & Carpenter, 1974). However, note that due to the instability of the zinc-free oligomer, the value of the microscopic dissociation constant is uncertain (Blundell et al., 1972). Steiner et al. (1975) propose that the connecting C peptide in proinsulin is oriented externally in such a way that the interprotomer interactions in the proinsulin hexamer are essentially the same as those present in $(In)_6(Zn^{2+})_2$.

On the basis of sequence homology and the lengths of the human proinsulin and the mouse β-NGF chains (81 and 118 amino acids, respectively), Frazier et al. (1972) proposed that the β-NGF gene evolved from a common ancestral proinsulin gene via gene duplication, fusion, and mutation. In their comparison of sequences, Frazier et al. (1972) assigned His-B10 in the proinsulin sequence and His-8 in the β-NGF sequence homologous positions before it was discovered that 7S NGF_n is a zinc metalloprotein.

In view of the sequence homology between insulin and β-NGF, and the similarities in biological function (Server & Shooter, 1977; Frazier et al., 1972), we have initiated investigations to compare the structural and chemical properties of the zinc ions in 7S NGF_n and $(In)_6(Zn^{2+})_2$. In this paper the chromophoric tridentate chelator 2,2′,2″-terpyridine (Terpy), in combination with rapid kinetic techniques, has been

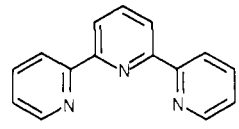

Terpy

used as a probe to investigate the microscopic environments about zinc ion in these two zinc metalloproteins. As will be shown, the kinetics and spectral changes that accompany the sequestering and removal of zinc ion by Terpy indicate highly similar modes of interaction between protein and metal ion for these two proteins.

Experimental Section

Materials. Insulin (bovine, crystalline), carboxypeptidases A and B (DFP treated), carbonic anhydrase, thermolysin, 2,2′,2″-terpyridine, Tris base, and Sephadex G-100 were purchased from Sigma Chemical Co. Horse liver alcohol dehydrogenase was purchased from Boehringer Mannheim and was prepared as previously described (Bernhard et al., 1970). Zn(II) (as the certified atomic absorption standard) was purchased from Fischer Scientific. Chelex 100 (100–200 mesh) was purchased from Bio-Rad. 7S NGF_n was prepared according to the procedure of Varon et al. (1967) from the submaxillaries of Swiss–Webster adult male mice (>35 g).

Methods. Insulin stock solutions (5 mg/mL) were prepared by mixing the crystalline protein with pH 8.00 Tris-HCl buffer (0.05 M) and then adjusting the solution to pH 10.5 with dilute NaOH to completely dissolve the protein. After readjusting the pH to 8.00, the solution was passed over a Chelex 100 column (40 × 1 cm) to remove all traces of zinc ion and other contaminating metal ions. Then Zn(II) was added as required just prior to use in the various experiments described under Results.

Solutions of carboxypeptidases A and B, carbonic anhydrase, thermolysin, and horse liver alcohol dehydrogenase were prepared by dissolving the proteins in 0.05 M Tris–$HClO_4$ buffer, pH 8.0, at a concentration of 0.6 mg/mL. Aliquots of 2.0 mL were treated with approximately 2 mL wet bed volume of Chelex 100 resin at room temperature for 10 min with periodic mixing. The resin was then separated by centrifugation in a conical tube, and the supernatant protein solution was removed. The reaction of these proteins with Terpy was examined by difference spectroscopy using a Cary 118C UV–visible recording spectrophotometer as described in the legend to Figure 1.

The stopped-flow rapid-mixing studies were performed with a computerized Durrum-Gibson D-110 spectrophotometer (dead time ~3 ms) equipped with a 2-cm light path observation cuvette. All of the stopped-flow kinetic studies were carried out with a 1.0-mm slit with an electronic time constant ≤ 0.5 ms. The computer was run under the control of an interactive FORTRAN program which allows the user to send, analyze, and store the data. In addition, the program permits the user to plot the observed time course and the theoretical fits on an x–y plotter interfaced to the computer [some of the details of the software and hardware for this system are described elsewhere (Dunn et al., 1979)].

Amplitude measurements and determination of the kinetic time course of the slow phase for the reaction of Terpy with 7S NGF_n were performed with a Varian 635 UV–visible spectrophotometer. Spectra were recorded with a Cary 118C UV–visible recording spectrophotometer. The metal ion content of the various protein preparations was determined either via atomic absorption or via titration with Terpy (Pattison & Dunn, 1975, 1976a).

The following extinction coefficients were used to determine concentrations: 7S NGF_n, $\epsilon_{280} = 2.15 \times 10^5$ M^{-1} cm^{-1} [Server & Shooter (1976); assuming a M_r of 137 000]; insulin (protomers), $\epsilon_{280} = 5.7 \times 10^3$ M^{-1} cm^{-1} (Porter, 1953); Terpy, $\epsilon_{290} = 1.60 \times 10^4$ M^{-1} cm^{-1}; mono(Terpy)–Zn(II) complex, $\epsilon_{317} = 2.2 \times 10^4$ M^{-1} cm^{-1} and $\epsilon_{330} = 2.3 \times 10^4$ M^{-1} cm^{-1}; bis-(Terpy)–Zn(II) complex, $\epsilon_{320} = 3.9 \times 10^4$ M^{-1} cm^{-1} and $\epsilon_{333} = 4.1 \times 10^4$ M^{-1} cm^{-1} (Holyer et al., 1966).

Results

Reaction of Terpy with 7S NGF. The reaction of excess Terpy with 7S NGF_n ultimately results in the formation of $Zn(Terpy)_2^{2+}$ and 7S NGF_a (Pattison & Dunn, 1976a,b). The reaction time course, measured at 332 nm, occurs via a two-step process. Typical time courses for the fast step (measured in a rapid-mixing stopped-flow apparatus) and for the slow step (measured in a conventional spectrophotometer) are shown respectively in parts A and B of Figure 1. The time-dependent spectral changes are presented as difference spectra in Figure 1C. Note that the spectrum of the product formed in the fast phase of the reaction (trace 2; λ_{max} 318 and 330 nm) is quite similar to the spectrum of a mono(Terpy)–Zn(II) complex and the spectrum of the final product is identical with the spectrum of a bis(Terpy)–Zn(II) complex (Pattison & Dunn, 1976a; Holyer et al., 1966). Note that the two steps occur on quite different time scales under the reaction conditions of Figure 1 (i.e., milliseconds and minutes). Since the processes are well separated, the time course for each step was found to be satisfactorily fit to the rate expression for a single first-order process (eq 1); i.e.

$$OD_t = OD_\infty - A_{exp}(-k_i t) \quad (1)$$

where A is the amplitude, k_i is the observed rate constant, i = 1 designates the fast step, and i = 2 designates the slow step. The magnitude of the apparent first-order rate constant, k_1, was found to be proportional to the concentration of Terpy (Figure 2A), and therefore the fast phase of the reaction

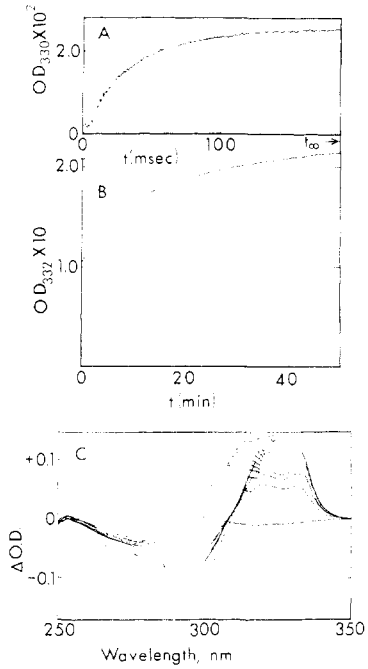

FIGURE 1: Kinetic time courses for the optical density changes accompanying the reaction of 2,2′,2″-terpyridine with 7S NGF_n. The rapid phase of the reaction (A) was measured in a stopped-flow rapid-mixing apparatus. The slow phase (B) and the difference spectra in (C) were measured with a conventional spectrophotometer. Conditions after mixing (A): Terpy, 50 μM; 7S NGF_n, ~0.4 μM; pH 7.40 Tris-HCl buffer, 0.05 M, 25.0 ± 0.5 °C. Conditions after mixing (B): Terpy, 50 μM; 7S NGF_n, ~3 μM; pH 7.40 Tris-HCl buffer, 0.05 M, 25.0 ± 0.5 °C. The kinetic run in (B) was initiated by the addition of Terpy following incubation of 7S NGF_n at the final dilution for 1 h. The first OD measurement in (B) corresponds to ~20 s after the addition of Terpy. The t_∞ OD in (B) is indicated on the right margin. (C) The difference spectra were obtained on mixing 7S NGF_n with Terpy in a double difference cuvette at 25.0 ± 0.2 °C in pH 6.86 sodium phosphate buffer, ionic strength 0.05. The reference cuvette contained identical solutions of 7S NGF_n and Terpy (unmixed). Trace 1 is the base line obtained prior to the mixing of the sample cuvette. Traces 2–10, respectively, were obtained at ~30 s, 3 min, 5 min, 7 min, 12 min, 20 min, 35 min, 60 min, and 14 h after mixing. Concentrations after mixing: 7S NGF_n, ~1.8 μM; Terpy, 0.1 mM (cuvette path length 0.872 cm).

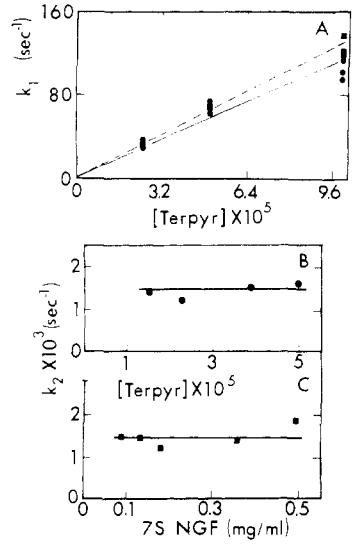

FIGURE 2: Concentration dependencies of the fast and slow steps of the Terpy–7S NGF_n reaction. (A) Comparison of the apparent rate constants (k_1) for the reactions of Terpy with 7S NGF_n (●, —) and with the aquo zinc ion (■, - - -). These stopped-flow rapid-mixing studies were carried out as described in Figure 1A. Terpy concentrations after mixing: 25, 50, and 100 μM. (B) Dependence of the apparent first-order rate constant for the slow step (k_2) on the concentration of Terpy. Measurements were carried out as described in Figure 1B. Terpy concentrations: 15, 22, 38, and 50 μM. (C) Dependence of k_2 on the concentration of 7S NGF_n. 7S NGF_n concentrations: 0.08, 1.3, 1.8, 3.5, and 5.0 mg/mL; pH 7.40 Tris-HCl buffer, 0.05 M, 25.0 ± 0.5 °C.

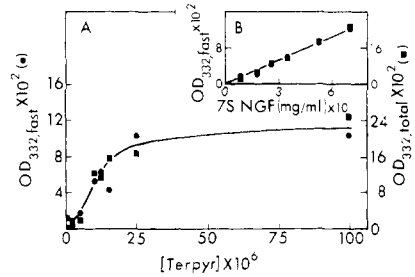

FIGURE 3: Comparison of the fast-step amplitude to the total amplitude of the Terpy–7S NGF_n reaction as a function of the Terpy concentration (A) and the 7S NGF_n concentration (B). Conditions: (A) 7S NGF_n, ~4 μM; variable Terpy; (B) Terpy, 50 μM; variable 7S NGF_n.

appears to be second order overall: first order with respect to Terpy and first order with respect to 7S NGF bound zinc ions. The slope of the best fit straight line in Figure 2A yields a second-order rate constant of 1.1×10^6 M^{-1} s^{-1}. Note that this value is similar to the rate constant for the reaction of Terpy with the aquated zinc ion, 1.3×10^6 M^{-1} s^{-1} (viz., Figure 2A). Holyer et al. (1966) report a value of 1.1×10^6 M^{-1} s^{-1} for the reaction of Terpy with the aquated zinc ion.

Over the range of 7S NGF_n and Terpy concentrations investigated, the apparent first-order rate constant for the slow step is concentration independent and therefore zero order with respect to the concentrations of both Terpy and 7S NGF_n (parts B and C of Figure 2). Within the limits of experimental error ($\pm 0.4 \times 10^{-3}$ s^{-1}) the rate constant for the slow step is identical with the rate constant for the appearance of 7S NGF_a proteolytic activity under these same conditions (Pattison & Dunn, 1976a,b).

Amplitude analyses of the reaction between Terpy and 7S NGF_n (Figure 3A) show that each step of the biphasic time course corresponds to approximately half of the total spectral change. Note that both the amplitude of the fast step and the amplitude of the total spectral change exhibit the same sigmoidal dependence on the total Terpy concentration. The Hill coefficient, here used as a measure of sigmoidicity, has a value of $n = 1.8 \pm 0.3$. Note also that the amplitudes of both steps exhibit the same linear dependence on protein concentration (Figure 3B).

Reaction of Terpy with the Zn(II)–Insulin System. Due to the lower affinity for Zn(II) and to the somewhat weaker interprotomer interactions exhibited by $(In)_6(Zn^{2+})_2$ in comparison to 7S NGF_n (Blundell et al., 1972; Pattison & Dunn, 1976a,b; Au & Dunn, 1977), experimental conditions which optimize the formation of the $(In)_6(Zn^{2+})_2$ species were selected for the study of the reaction of Terpy with the insulin-bound zinc ion. The studies of Fredericq (1956) indicate that hexamer formation is optimal in the pH region 7–9. Due to the presence of one or more relatively weak (additional) zinc ion binding sites, ratios of $[Zn^{2+}]/[In] \gg 0.33$ result in the formation of insulin–Zn^{2+} oligomers (polymers) larger than the hexamer that contain more than 2 g-atoms of Zn^{2+} per 6 insulin monomers (Blundell et al., 1972). Therefore, except where noted, the studies described below were carried out under conditions where $[Zn^{2+}]/[In] \leq 0.3$.

Typical stopped-flow traces for the reaction of Terpy with insulin-bound Zn(II) ion, under conditions where the

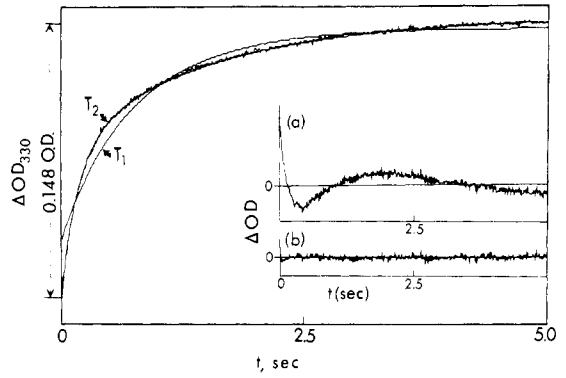

FIGURE 4: Stopped-flow rapid-mixing kinetic time courses for the reaction of Terpy with the Zn(II)–insulin system. T_1 and T_2 refer, respectively, to the computer best fit theoretical time courses (smooth traces) for a first-order process and for two sequential first-order processes (see Methods and Results). Note that the theoretical time courses are overlaid on the experimentally observed time course (noisy trace). The insets to each figure are difference plots of the theoretical minus the observed time courses for (a) a first-order process and (b) two sequential first-order processes. Concentrations after mixing: Terpy, 500 μM; In (monomers), 75 μM, and $Zn(NO_3)_2$, 4.8 μM; pH 8.00 Tris-HCl buffer, 0.05 M, 25.0 ± 0.5 °C. Wavelength was 330 nm. Best fit kinetic parameters (trace T_1): A = 0.111 OD; k = 1.12 s^{-1}; χ_ν^2 = 23.4. Best fit kinetic parameters (trace T_2): A_1 = 0.0789 OD; k_1 = 5.26 s^{-1}; A_2 = 0.0692 OD; k_2 = 0.601 s^{-1}; χ_ν^2 = 1.29.

$[Zn^{2+}]/[In] = 0.178$ and $[Terpy]_0 \gg [Zn^{2+}]_0$, are shown in Figure 4. Under these conditions, the Terpy optical density changes are biphasic in appearance. It was found that the complete reaction time courses could not be satisfactorily fit to the rate expression for a single, first-order process. However, the OD changes are satisfactorily fit by mechanisms involving either two sequential apparent first-order processes (eq 2)

$$A + B \xrightarrow{k_1} x \xrightarrow{k_2} y \qquad [B] \gg [A] \qquad (2)$$

or two simultaneous apparent first-order processes (eq 3)

$$A + B \xrightarrow{k_1} x \quad [B] \gg [A] \qquad (3)$$

$$A + B \xrightarrow{k_1} y \quad [B] \gg [A]$$

Note that the best fit theoretical time courses in Figure 4a for the rate laws corresponding to eq 2 (trace T_1) and eq 3 (trace T_2) are overlaid on the experimentally observed time course. The insets to Figure 4a present the difference between the theoretical time courses and the experimentally observed time course. These data clearly show that the time course is biphasic.

So long as $k_1 > k_2$ and $A_1 \simeq A_2$, the best fit (see Experimental Section) rate constants and amplitudes for these two mechanisms were very nearly identical and yielded identical reduced χ^2 values. Under conditions where k_1 is only two- to threefold greater than k_2 and $A_1 \ll A_2$ (i.e., at relatively low Terpy concentrations), fitting the data from the same trace to either of these two mechanisms yielded identical rate constants but slightly different relative amplitudes. Hence, the computer fitting did not provide a basis for distinguishing between simultaneous and sequential reaction mechanisms for the biphasic time courses.

Assuming a sequential reaction mechanism, Figure 5 summarizes the dependence of the amplitudes and the apparent first-order rates of the fast and slow steps for the reaction of Terpy with insulin-bound Zn(II). These data indicate that the rate of the fast step is proportional to the concentration of Terpy (Figure 5A), while the apparent first-order rate constant for the slow step is proportional to the concentration

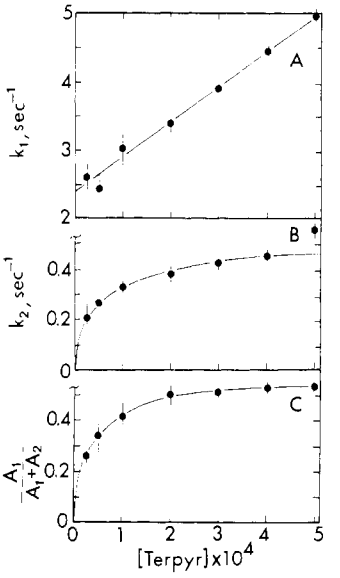

FIGURE 5: Comparison of concentration dependencies of the observed rate constants and amplitudes for the biphasic reactions of Terpy with the Zn(II)–insulin system. The experimental conditions were the same as those described in Figure 4. The kinetic parameters were obtained as described in Figure 4 and the text (see Methods and Discussion and Conclusions). The slope and intercept of the best fit straight line in (A) are slope = 5.1 × 10^3 M^{-1} s^{-1} and intercept = 2.4 s^{-1}. The curves in (B) and (C) were drawn assuming hyperbolic dependencies. The best fit rate constants ($k_{2,sat}$) or amplitude ratios extrapolated to infinite [Terpy] and the best fit hyperbolic constants (K) are as follows: (B) K = 4.9 × 10^{-5} M and $k_{2,sat}$ = 0.6 s^{-1}; (C) K = 4.1 × 10^{-5} M and $[(A_1)/(A_1 + A_2)]_{sat}$ = 0.61.

of Terpy at low concentrations and tends toward a limiting saturated value at high concentrations. Note that extrapolation of the best fit straight line for the Zn(II)–insulin system to the ordinate intercept (Figure 5) yields a finite, positive value of ~2 s^{-1}. Consequently, the fast step appears to involve a reversible binding reaction that is second order in the forward direction and first order in the reverse direction. The slow step (Figure 5B) appears to be a true, quasi-irreversible first-order process that is coupled to the faster reversible step. At high (saturating) Terpy concentrations, the slow step becomes zero order with respect to Terpy.

The sum of the amplitudes for the fast and slow steps (i.e., the total amplitude) remains constant over the range of Terpy concentrations investigated. However, the relative magnitudes vary (Figure 5C). As the Terpy concentration increases, the fraction of total OD change occurring in the fast phase varies from approximately 0.25 to a saturated value approaching 0.5 to 0.6. Note that the level of uncertainty associated with measurement of amplitudes (and rates) increases at the low Terpy concentrations because $A_1 \ll A_2$ and $k_1 \simeq k_2$ under these conditions.

For determination of whether or not the biphasic reaction time course results from the presence of more than one zinc ion species preexisting in solution, the dependence of rates and relative amplitudes on the $[Zn^{2+}]/[In]$ ratio was investigated in detail. The results of these studies are summarized in Figure 6. When the $[Zn^{2+}]/[In]$ is ≤0.3, the observed time courses at high Terpy concentration are biphasic and the ratio of the amplitudes $A_1/(A_1 + A_2) \simeq 0.60$, and apparent first-order rate constants for the two phases are invariant. For $[Zn^{2+}]/[In]$ ratios > 0.3, the time courses (data not shown) appear to be triphasic. The apparent first-order rate constants and the amplitudes associated with the second and third phases correspond in magnitude to the rates and amplitudes of the biphasic time courses obtained when $[Zn^{2+}]/[In] \leq 0.3$. Note

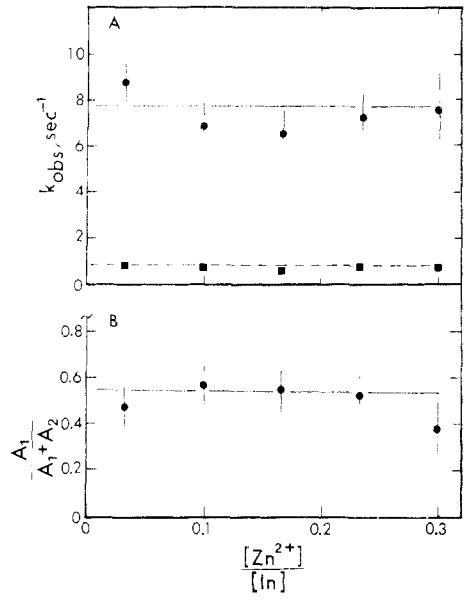

FIGURE 6: Dependence of apparent rate constants (A) and amplitudes (B) characterizing the biphasic time course for the reaction of Terpy with the Zn(II)–insulin system in 0.05 M pH 8.00 Tris-HCl buffer at 25.0 ± 0.2 °C. The data were obtained as described in Figure 4 by using similar conditions: Terpy, 0.4 mM; In (nonomers), 75 μM; $Zn(NO_3)_2$, variable.

that the apparent first-order rate constant of the first phase of the triphasic time course is approximately 10-fold greater than that of the second phase.

In order to compare the spectral changes occurring in the two phases of the reaction, the dependence of relative amplitudes on wavelength was examined; at a $[Zn^{2+}]/[In]$ ratio of 0.167 and a [Terpy] = 4.0×10^{-4} M (i.e., the conditions of Figure 5), the ratio $A_1/(A_1 + A_2)$ was found to be essentially independent of wavelength in the spectral region 320–340 nm (data not shown).

The molecular weight properties of the insulin species generated for $[Zn^{2+}]/[In]$ ratios varied between 0.066 and 0.33 were investigated via gel filtration chromatography. In these experiments, 2-mL samples initially containing 0.7 mM In and varying concentrations of Zn(II) in 0.05 M pH 8.00 Tris-HCl buffer at room temperature were chromatographed over a 52.5 × 2.2 cm column of Sephadex G-100 equilibrated with the same buffer. Samples containing [Zn]/[In] ratios of 0.066, 0.165, and 0.231 eluted in two well-separated peaks (see Table I). The sample containing a [Zn]/[In] ratio of 0.33 gave a single peak with a lower molecular weight shoulder (Table I). By comparison of elution volumes with molecular weight standards, average apparent molecular weights of 36 000 ± 4000 and 13 000 ± 2000 were found for the two peaks (viz., Table I). The apparent average molecular weights were determined via a plot of log M_r vs. K_{av}, where $K_{av} = (V_e - V_0)/(V_t - V_0)$, V_e = sample elution volume, V_0 = blue dextran elution volume, and V_t = total gel bed volume. The results summarized in Table I indicate that the major insulin species present in these solutions are the insulin dimer and the insulin hexamer. Note that the amount of hexamer formed is a function of the amount of zinc ion present. Quantitation of the amount of zinc eluting from each column run shows that essentially all (at least 90%) of the zinc applied to the column coelutes with protein in the 36 000 molecular weight peak. Finally, in each column run a very small amount of protein (see Table I) was observed to elute with a molecular weight ≤6000. This material was assumed to be either insulin monomer or insulin fragments. These results are in accord with the monomer–dimer–hexamer model for the assembly of $(In)_6(Zn^{2+})_2$ [see Blundell et al. (1972)].

Reaction of Terpy with Other Zinc Metalloproteins of Known Three-Dimensional Structure. The reactions of Terpy with carboxypeptidases A and B, carbonic anhydrase, thermolysin, and horse liver alcohol dehydrogenase were found to be very slow with a reaction time course of hours to days. In all cases the reaction could be described by a single exponential.

Discussion and Conclusions

The kinetics and spectral changes which characterize the reaction of Terpy with divalent metal ions in aqueous solution have been studied in some detail (Holyer et al., 1966). The reaction of an excess of Terpy with the aquated zinc ion results in the rapid formation of a strongly absorbing bis complex ($\epsilon_{333} = 4.1 \times 10^4$ M^{-1} cm^{-1} and $\epsilon_{320} = 3.90 \times 10^4$ M^{-1} cm^{-1}). The rate of formation of the bis complex is limited by the rate of substitution of Terpy for inner sphere coordinated water to form the mono complex (eq 4):

$$\begin{array}{ccc} Zn(H_2O)_6^{2+} + Terpy \overset{slow}{\rightleftharpoons} Zn(H_2O)_5(Terpy)^{2+} + 3H_2O & & \\ \Big\downarrow{\scriptstyle Terpy,\ fast} & & \\ Zn(Terpy)_2^{2+} + 3H_2O & & \end{array} \quad (4)$$

At 25 °C and neutral pH, the reaction is characterized by a rate constant of 1.1×10^6 M^{-1} s^{-1} (Holyer et al., 1966). This rate constant is indicative of a rate-limiting loss of water from the inner sphere coordination shell.

The mono complex ($\epsilon_{330} = 2.3 \times 10^4$ M^{-1} cm^{-1}; $\epsilon_{317} = 2.2 \times 10^4$ M^{-1} cm^{-1}) is formed in aqueous solution when $[Zn^{2+}] \gg$ [Terpy]. It is of considerable importance to this work to note that the long-wavelength absorption bands of the bis complex are approximately twice as intense as those of the mono complex and that the maxima in the two spectra occur at nearly identical wavelengths.

In contrast, the reactions of Terpy with the zinc ions of 7S NGF and $(In)_6(Zn^{2+})_2$, as demonstrated in these studies, follow markedly biphasic time courses (viz., Figures 1 and 4). The spectrum of the product formed in the fast phase of the 7S NGF_n–Terpy reaction (Figure 1C) corresponds to a mono(Terpy)–Zn(II) complex. The spectrum of the final product is identical with the spectrum of the bis(Terpy)–Zn(II) complex. The wavelength independence of reaction amplitudes for the Terpy–$(In)_6(Zn^{2+})_2$ system (data not shown) indicates that each phase of the biphasic reaction corresponds to the inner sphere coordination of Terpy to zinc ion. The data presented in Figure 6 and the gel filtration chromatography study provide strong evidence that for $[Zn^{2+}]/[In]$ ratios ≤0.3 the $(In)_6(Zn^{2+})_2$ species is the only stoichiometrically important zinc-containing species present in solution. This finding is in accord with the results derived from a wide variety of techniques (i.e., equilibrium dialysis, light scattering, and ultracentrifugation) used in other laboratories to investigate the assembly of $(In)_6(Zn^{2+})_2$ [see Blundell et al. (1972) for a review of this subject]. These data clearly demonstrate that the assembly of the hexameric species is a highly cooperative process in the presence of zinc ion.

For both of the metalloprotein hormones here considered, the second-order rate constant which characterizes the fast phase of the reaction is similar in magnitude, but not identical, to the corresponding rate constant for the reaction of Terpy with the aquated zinc ion. These less than diffusion-limited processes could represent either the sterically restricted rate of diffusion of Terpy to the protein-bound metal ion, as shown in eq 5, or the rate of inner sphere substitution from a weak

Scheme I: Model of the Zinc-Insulin Hexamer Showing the Arrangement of the Six Subunits, the Location of the Two Zinc Ions on the Threefold Symmetry Axis in the Central Cavity, and the Local Twofold Axes (Details of the Coordination of Zinc Ion Are Shown in the Upper Right-Hand Corner Viewed along the Threefold Symmetry Axis)

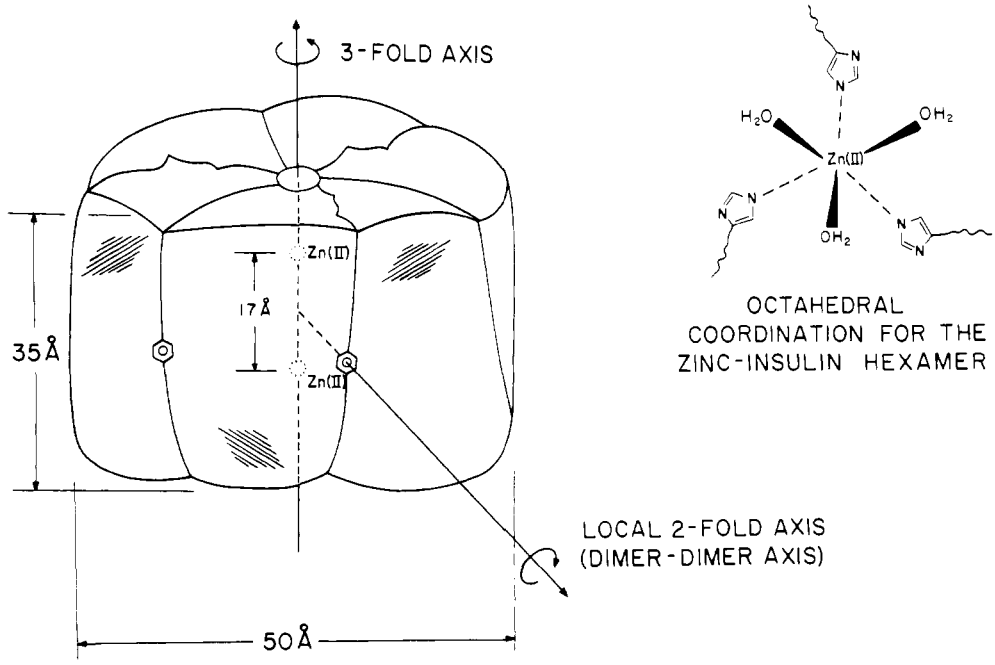

outer sphere complex (with a rate-limiting dissociation of the ligand, X), as shown in eq 6

$$\begin{array}{c} PZn(X)_3^{2+} \overset{\text{fast}}{\rightleftharpoons} PZn(X)_2^{2+} + X \\ \Big\downarrow \text{Terpy, slow} \\ PZn(Terpy)^{2+} + 2X \end{array} \quad (5)$$

$$\begin{array}{c} PZn(X)_3^{2+} + Terpy \overset{\text{fast}}{\rightleftharpoons} PZn(X)_3^{2+}(Terpy) \\ \Big\downarrow \text{slow} \\ PZn(Terpy)^{2+} + 3X \end{array} \quad (6)$$

where P = protein and X = solvent molecule or ion.

Although the spectral changes correspond to the formation of a Terpy–zinc ion complex in each system, the second phase of the reaction, by all criteria examined, exhibits the behavior of a true first-order process. Therefore, the rate at which complex formation occurs in the second step must be limited by a preceding, obligatory, unimolecular step. Since the final reaction products consist of the bis(Terpy)–zinc ion complex and the metal-ion-free protein, the most reasonable mechanism for the biphasic reactions involves the coordination of Terpy to the protein-bound zinc ion in the fast step, followed by a slow, rate-limiting dissociation of the Terpy-coordinated zinc ion from the protein (the unimolecular step) and the rapid coordination of a second Terpy molecule to form the bis-(Terpy)–zinc ion product as indicated in eq 7.

$$\begin{array}{c} PZn(OH_2)_3^{2+} + Terpy \overset{k_1,\ \text{fast}}{\rightleftharpoons} PZn(Terpy)^{2+} + 3H_2O \\ \Big\downarrow k_2, \text{ slow} \\ Zn(Terpy)_2^{2+} \overset{\text{Terpy}}{\underset{\text{fast}}{\rightleftharpoons}} Zn(Terpy)^{2+} + P \end{array} \quad (7)$$

Note that the amplitude changes which characterize the biphasic time courses are consistent with the formation of mono- and bis(Terpy)–zinc ion complexes, respectively, in the two phases of the reaction. Here it is assumed that the mono(Terpy)–zinc ion–protein complexes have spectra which are qualitatively and quantitatively similar to the simple mono(Terpy)–zinc ion complexes described by Holyer et al. (1966).

Indeed, the high-resolution X-ray structure of $(In)_6(Zn^{2+})_2$ is fully consistent with the mechanism described by eq 7. $(In)_6(Zn^{2+})_2$ is a bagel-shaped molecule with an approximate outside diameter of ~50 Å and a height of ~35 Å, as shown in Scheme I. The two zinc ions are located on the molecular threefold symmetry axis in a central, water-filled cavity that runs through the molecule. The zincs are separated by a distance of 17 Å and are situated ~9 Å from the surface of the protein. The three ligands contributed to each zinc ion by the protein (His-B10 residues) extend out into the central cavity. The remaining three ligands appear to be water molecules as determined by the distribution of electron densities in the high-resolution maps (Blundell et al., 1972). We conclude that the rapid phase of the reaction involves the displacement of the three water molecules to form a mono complex and the slow phase involves dissociation of the metal ion from the protein, followed by the rapid coordination of a second Terpy molecule, as postulated in eq 7. Therefore, the high-resolution X-ray structure provides a satisfying physicochemical rationale for the biphasic time course of the Terpy reaction.

The X-ray structures of carboxypeptidase A, thermolysin, carbonic anhydrase, and horse liver alcohol dehydrogenase have been determined and, in each case, the active-site zinc ion has been shown to be four coordinate [see Dunn (1975) for a review]. Three of the four inner sphere ligands are derived from amino acid side chains, while the fourth ligand is either a water molecule or hydroxide ion. In each case the ligands are arranged in a distorted tetrahedral array about the zinc ion with the water (or hydroxide ion) facing out into a cavity or cleft which forms the substrate binding site–active site region on the enzyme surface. Thus, the differences in the zinc ion binding geometries for these proteins vs. $(In)_6$-

Table I: Sephadex G-100 Chromatography of Insulin with Varying Amounts of Zinc

sample,[a] % hexamer	[Zn]/[In][b]	peak I, $M_{r,app}$ 36 000 ± 4000 % of sample[c] ± 3%	[Zn]/[In][d] ± 0.01	peak II, $M_{r,app}$ 13 000 ± 2000 % of sample[c] ± 3%	[Zn]/[In][d] ± 0.001	loss[e] % of sample ± 3%
10	0.033	12.7	0.32	82.4	0.039	4.9
20	0.066	18.9	0.31	79.2	0.065	1.9
50	0.165	51.0	0.31	48.5	0.065	0.5
70	0.231	66.3	0.37	31.9	0.102	1.8
100	0.33	88.9	0.31			11.1[f]

[a] Samples were prepared from metal-free insulin and the [In] was determined from the absorbance at 280 nm. The zinc was added 10 min prior to the start of chromatography. The percent hexamer is the percent of the insulin which should have been in the hexamer form based on the amount of added zinc assuming a stoichiometry of $(In)_6(Zn^{2+})_2$. [b] The [Zn]/[In] was calculated from the initial [In] and the quantity of zinc added. [c] The percent of sample in each peak was determined from the 280-nm absorbance of the fractions in that peak and the known 280-nm absorbance of the applied sample. [d] The zinc concentration in each peak was determined via titration with Terpy as described under Methods. [e] The percent loss is the quantity of 280-nm absorbance not eluting in peaks I and II. This material was accounted for in fractions with apparent molecular weight ≤6000. [f] Most of this material is accounted for as protein in a shoulder to the 36 000 M_r peak.

$(Zn^{2+})_2$ are reflected in the markedly different time courses for the sequestering and removal of zinc ion from these proteins by Terpy.

Note that Terpy is an obligate planar tridentate ligand (Cotton & Wilkinson, 1972; Einstein & Penfold, 1966). Consequently, the characteristic UV–visible spectrum of Terpy–zinc complexes would be significantly altered if the Terpy pyridyl rings were forced to assume a nonplanar conformation by steric constraints imposed by other ligands. Therefore, complexation of Terpy to the protein-bound metal ions of 7S NGF_n and $(In)_6(Zn^{2+})_2$ must result in the formation of Terpy–Zn^{2+}–protein complexes with meridional coordination (such as I or II) rather than facial coordination (III). Since the zinc ions of crystalline $(In)_6(Zn^{2+})_2$ reside on the molecular threefold axis, formation of a complex with meridional coordination could occur only via rearrangement of the insulin ligands and/or dissociation of one of the protein ligands (eq 8):

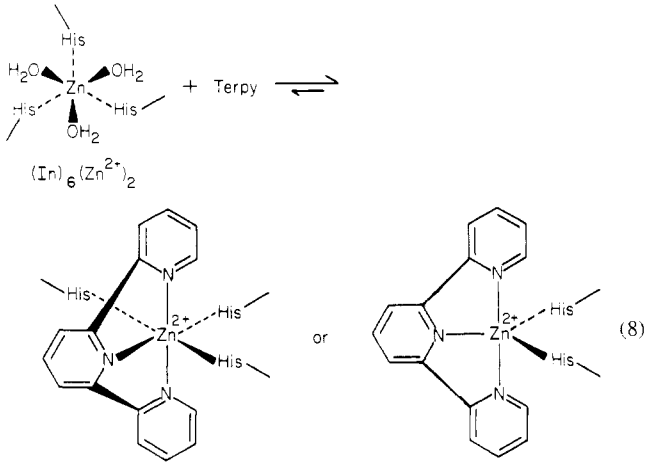

I, meridional hexacoordinate complex

II, meridional pentacoordinate complex

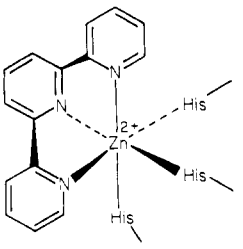

III, facial hexacoordinate complex

The striking similarities between the reactions of Terpy with $(In)_6(Zn^{2+})_2$ and 7S NGF_n suggest a common mechanism. Hence, we postulate that the fast and slow phases of the Terpy–7S NGF_n reaction also occur via the mechanism described in eq 7.

On the basis of the circumstantial evidence presented in this study, together with the assignment of homologous positions to His-B10 of In and His-8 of the NGF β chain, it is tempting to postulate the existence of structural homology between the 7S NGF_n and $(In)_6(Zn^{2+})_2$ zinc binding sites. Any such structural homology would predict a similarity of biological roles for zinc ion in these two zinc metalloprotein hormones. Verification of this hypothesis must await the accumulation of further information concerning the structure and function of the zinc sites on 7S NGF_n.

Acknowledgments

The authors thank Richard Wing for contributions in the form of theoretical discussions and Steven C. Koerber and Richard G. Morris for advice and assistance with the computer software programs used in these studies.

References

Angeletti, R. H., & Bradshaw, R. A. (1971) *Proc. Natl. Acad. Sci. U.S.A. 68*, 2417.

Au, A. M.-J., & Dunn, M. F. (1977) *Biochemistry 16*, 3958.

Bernhard, S. A., Dunn, M. F., Luisi, P. L., & Schack, P. (1970) *Biochemistry 9*, 185.

Blundell, T., Dodson, G., Hodgkin, D., & Mercola, D. (1972) *Adv. Protein Chem. 26*, 279.

Cotton, F. A., & Wilkinson, G. (1972) in *Advanced Inorganic Chemistry*, 3rd ed., pp 622–625, Wiley-Interscience, New York.

Dunn, M. F. (1975) *Struct. Bonding (Berlin) 23*, 61–122.

Dunn, M. F., Bernhard, S. A., Anderson, D., Copeland, A., Morris, R. G., & Roque, J.-P. (1979) *Biochemistry 18*, 2346.

Einstein, F. W. B., & Penfold, B. R. (1966) *Acta Crystallogr. 20*, 924.

Frank, B. H., & Veros, A. J. (1970) *Biochem. Biophys. Res. Commun. 38*, 284.

Frazier, W. A., Angeletti, R. H., & Bradshaw, R. A. (1972) *Science 176*, 482.

Fredericq, E. (1956) *Arch. Biochem. Biophys. 65*, 218.

Goldman, J., & Carpenter, F. H. (1974) *Biochemistry 13*, 4566.

Grant, P. T., Coombs, T. L., Thomas, N. W., & Sargent, J. R. (1971) in *Subcellular Organisation and Function in Endocrine Tissues* (Heller, H., & Lederis, K., Eds.) p 481,

Cambridge University Press, London and New York.
Holyer, R. H., Hubbard, C. D., Kettle, S. F. A., & Wilkins, R. G. (1966) *Inorg. Chem. 5*, 622.
Jeffrey, P. D. (1974) *Biochemistry 13*, 4441.
Pattison, S. E., & Dunn, M. F. (1975) *Biochemistry 14*, 2733.
Pattison, S. E., & Dunn, M. F. (1976a) *Biochemistry 15*, 3691.
Pattison, S. E., & Dunn, M. F. (1976b) *Biochemistry 15*, 3696.
Pekar, A. H., & Frank, B. H. (1972) *Biochemistry 11*, 4013.
Porter, R. R. (1953) *Biochem. J. 53*, 320.
Server, A. C., & Shooter, E. M. (1976) *J. Biol. Chem. 251*, 165.
Server, A. C., & Shooter, E. M. (1977) *Adv. Protein Chem. 31*, 339.
Steiner, D. F., Kemmler, W., Tager, H. S., Rubenstein, A. H., Lernmark, Å., & Zühlke, H. (1975) *Cold Spring Harbor Conf. Cell Proliferation 2*, 531-549.
Varon, S., Nomura, J., & Shooter, E. M. (1967) *Biochemistry 6*, 2202.

Evidence That Hydride Transfer Precedes Proton Transfer in the Liver Alcohol Dehydrogenase Catalyzed Reduction of *trans*-4-(*N*,*N*-Dimethylamino)cinnamaldehyde†

Richard G. Morris,‡ Gerald Saliman,§ and Michael F. Dunn*

ABSTRACT: The kinetics of the decay of enzyme-bound intermediate to products for the horse liver alcohol dehydrogenase (LADH) catalyed reduction of *trans*-4-(*N*,*N*-dimethylamino)cinnamaldehyde (DACA) by NADH as a function of pH are reported. The intermediate has previously been shown to be an E(NADH,aldehyde) complex involving inner-sphere coordination of the carbonyl oxygen of DACA to the active-site zinc ion [Dunn, M. F., Biellman, J.-F., & Branlant, G. (1975) *Biochemistry 14*, 3176]. The reaction was carried out in the presence of 20 mM pyrazole, a potent LADH inhibitor, to drive the reaction to completion via formation of the LADH-NAD-pyrazole adduct. Under conditions of $[DACA]_0$, $[E]_0 \gg [NADH]_0$, intermediate decay was found to be an apparent first-order process over the pH range 4.33-9.00. The decay of the intensely chromophoric intermediate was found to be markedly pH dependent. Under conditions of rate saturation (i.e., when $[DACA]_0$, $[E]_0 \gg K_D$, the apparent dissociation constant for the intermediate), the decay rate was found to decrease with increasing pH. Substitution of (4*R*)-4-deuterionicotinamide adenine dinucleotide (NADD) for NADH gave a primary kinetic isotope effect of 2.8 at pH 4.33. The isotope effect decreases with increasing pH and was found to be $\simeq 1.0$ above pH 7. Analysis of the pH-rate profiles for NADH and NADD gave apparent pK_a values of 6.00 ± 0.20 and 6.51 ± 0.20, respectively. The pH-independent decay rate constants for NADH and NADD were 7.2 s^{-1} and 2.3 s^{-1}, respectively. The observed pH-independent spectrum of the intermediate and the pH dependencies of the decay process and the isotope effect could not be explained by mechanisms involving either a rapid preequilibrium protonation of the intermediate or a proton transfer concerted with hydride transfer. Although unlikely, a concerted mechanism involving an as yet undetected proton transfer via a protonic enzyme residue with $pK_a > 10.6$ could not be ruled out. The simplest mechanism that predicts both the pH dependencies of the isotope effect and the decay rates and explains the pH-independent spectrum of the intermediate involves (1) aldehyde activation for hydride attack via inner sphere coordination to zinc ion, (2) proton transfer to zinc-coordinated alcoholate ion in a step subsequent to hydride transfer, and (3) release of products from the site.

Previous studies from this laboratory (Dunn & Hutchison, 1973; Dunn et al., 1975; Angelis et al., 1977; Dunn et al., 1977) have shown that a transient chemical intermediate (λ_{max} 464 nm; ϵ_{max} 6.2×10^4 M^{-1} cm^{-1}) is formed during the liver alcohol dehydrogenase (LADH)[1] catalyzed reduction of 4-*trans*-(*N*,*N*-dimethylamino)cinnamaldehyde (λ_{max} 398 nm; ϵ_{max} 3.10×10^4 M^{-1} cm^{-1}), viz., Scheme I.

The intermediate (NADH)E(I) is formed in a rapid, reversible, and pH-independent step with $k_f = 4 \times 10^7$ M^{-1} s^{-1} and $k_r = 280$ s^{-1} (Dunn & Hutchison, 1973; Dunn et al., 1975). Preliminary studies (Dunn & Hutchison, 1973; Dunn et al., 1977) have shown that the rate of decay of the intermediate to products is markedly pH dependent; above pH 9, the intermediate is extremely long-lived, while, at lower pH values, the intermediate is a transient species. When the 1,4,5,6-tetrahydronicotinamide analogue of NADH (H_2NADH) is substituted for NADH, reaction yields a chromophore with a visible spectrum nearly identical with that of the intermediate (Dunn et al., 1975). This species is stable over a broad range of pH values. On the basis of these studies, a structure for the intermediate involving inner-sphere coordination of the carbonyl oxygen of DACA to the LADH active site zinc ion (Scheme II) was proposed.

Studies of model Lewis acid complexes with DACA and derivatives of DACA resulted in the formation of species with spectral properties remarkably similar to the spectrum of the

† From the Department of Biochemistry, University of California, Riverside, Riverside, California 92521. *Received April 3, 1979; revised manuscript received September 10, 1979.* This work was supported in part by the National Science Foundation, Grants GB 31151 and BMS 75-20339. A portion of these studies were carried out by R.G.M. in partial fulfillment of the Degree of Doctor of Philosophy.

‡ Present address: Dionex Corp., Sunnyvale, CA 94086.

§ Supported by the National Science Foundation Undergraduate Summer Research Program (GY 9922).

[1] Abbreviations used: DACA, *trans*-4-(*N*,*N*-dimethylamino)cinnamaldehyde; LADH, horse liver alcohol dehydrogenase; NAD^+, oxidized nicotinamide adenine dinucleotide; NADH, reduced nicotinamide adenine dinucleotide; NADD, (4*R*)-4-deuterionicotinamide adenine dinucleotide; H_2NADH, 1,4,5,6-tetrahydronicotinamide adenine dinucleotide; ADPR, adenosine diphosphoribose.

0006-2960/80/0419-0725$01.00/0